International Journal of Engineering Sciences & Emerging Technologies, May 2015.
ISSN: 22316604 Volume 7, Issue 6, pp: 766-777 ©IJESET

ANALYSIS OF PRESTRESSED CONCRETE CONTAINMENT VESSEL BY MODELLING REBARS AND TENDONS THROUGH MEMBRANE

S V Chaudhari[1], M A Chakrabarti[2]
[1]Department of Structural Engineering, VJTI, Matunga, Mumbai, India
[2] Department of Structural Engineering, VJTI, Matunga, Mumbai, India

ABSTRACT

This paper describes the nonlinear analysis of 1/8th portion of the 1:4 scaled model of prestressed concrete containment vessel using ABAQUS- a general purpose finite element analysis software. The reinforcing steel and the prestressing tendons are modelled through membrane rebar property. Concrete damaged plasticity, tension stiffening, plastic behaviour of reinforcing steel, liner and perstressing tendon are properly accounted for appropriate simulation of the nonlinear behaviour of these materials. The model is analysed for the internal pressure and the results are compared with LST results as documented in SNL- ISP-48 report.

KEYWORDS: *ABAQUS, Concrete Damaged Plasticity, Tension Stiffening, Rebar, Tendon*

I. INTRODUCTION

In our modern consumeristic power hungry generation the nuclear power plants play a very important role to meet the energy needs. However these plants are also equally dangerous because of their side effects in case of any leakages in an unfortunate accidental event. Therefore it has become very essential to perform the safety assessment of the nuclear reactor containment. The foremost important thing in any nuclear power plant is the nuclear reactor enclosed in the containment vessel. The shape of containment structure is commonly cylindrical with a dome as roof. These structures are planed very carefully and very meticulously designed by considering all possible loads and environmental hazards under the guidance of applicable code of conduct. Also, they are constructed under strict supervision. The containment structure is generally consisting of a primary containment vessel and a secondary containment vessel. It is common practice to construct the containment structures as the pre-stressed or post-tensioned structures.

Since late 1970 many attempts to capture the exact behaviour of the containment structure and its failure mechanisms were made in [1], [2], [3], [4], [5]. To understand the behaviour and the ultimate pressure capacity of the containment structure a large scale test was conducted on 1:4 scaled model of prestressed concrete containment vessel at Sandia National Laboratory, USA. It is also known as International Standard Problem No.48 [6]. A pre and post analysis was performed for this test as described in [7], [8], [9], [10]. With the evolution of new generation computers and well defined constitutive material models, the nonlinear finite element analysis of the containment structure resulted in better accuracy in behavioural prediction. In this paper the 1:4 scaled model of prestressed concrete containment vessel is modelled by considering its $1/8^{th}$ portion. The reinforcing steel and the prestressing tendons are modelled through membrane rebar property to simplify the geometric modelling process, which is the most time consuming and quite cumbersome. The material properties of reinforcing steel, presterssing tendon and concrete with proper constitutive models are given. Concrete damaged plasticity, tension stiffening, plastic behaviour of reinforcing steel, liner and perstressing tendon are properly accounted for appropriate simulation of the nonlinear behaviour of

these materials. The 1/8th model is analysed for the internal pressure and the results are compared with LST results as documented in SNL- ISP-48 report.

1.1. 1:4 Scaled Prestressed Concrete Containment Vessel:

The geometry of the model is as shown in the Figure 1. It consists of a basemat, a cylindrical wall and a dome above. For the present study a 1/8th (i.e. 45^0) 3D finite element model of 1:4 scaled PCCV model is prepared using ABAQUS a general finite element analysis software.

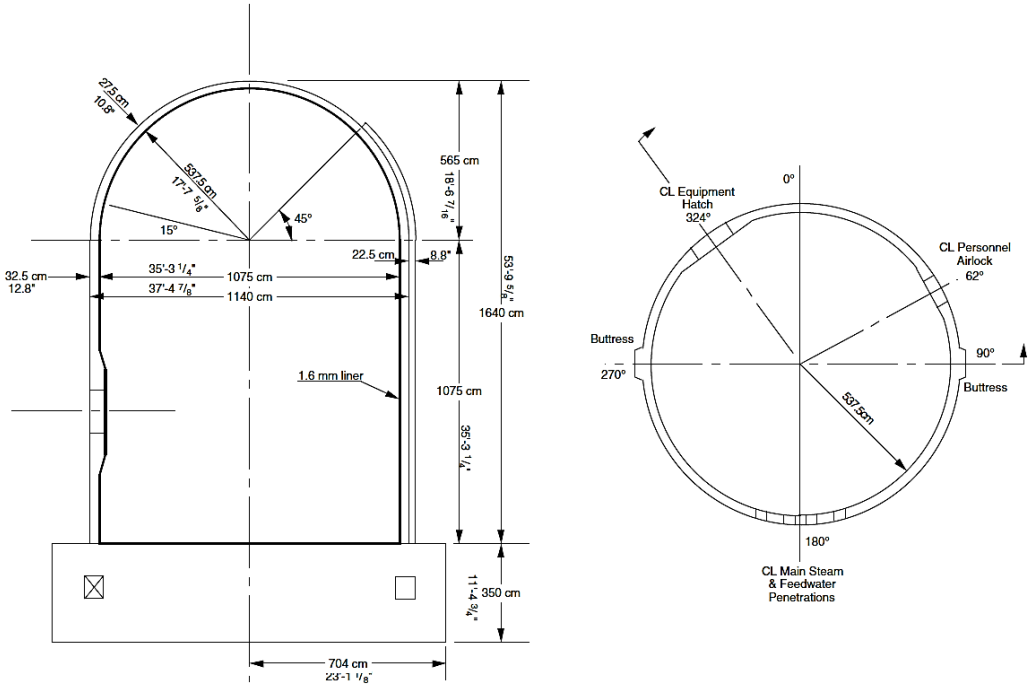

Figure 1. The 1:4 scaled PCCV model [9]

II. MATERIALS AND METHODS

The properties of the materials used in the 1:4 scaled PCCV model tested at Sandia National Laboratory, USA, are taken for the analysis. The material modelling and properties for concrete, rebars, prestressing steel and liner steel used are as follow.

2.1 Concrete:

Concrete shows highly nonlinear behaviour under tension as well as under compression, due to cracking and plasticity respectively. The material nonlinearity due to tension plays major role than that of due to compression in the failure of the containment structure subjected to internal pressure. The concrete is modelled using Concrete Damaged Plasticity Model in ABAQUS.

2.1.1 Concrete Damaged plasticity:

Under low confining pressures, concrete behaves in a very brittle manner and therefore the main failure mechanisms are cracking in tension and crushing in compression. The brittle behaviour of concrete vanishes when the confined pressure in concrete is adequately large to prevent crack. The damage in quasi-brittle materials can be defined by equating the dissipated fracture energy required to generate micro cracks [11].

These two main failure mechanisms, the tensile cracking and compressive crushing, are taken into account in this model. The evolution of the yield (or failure) surface is controlled by two hardening variables, $\tilde{\varepsilon}_c^{pl}$, linked to failure mechanisms under tension and compression loading, respectively [12].

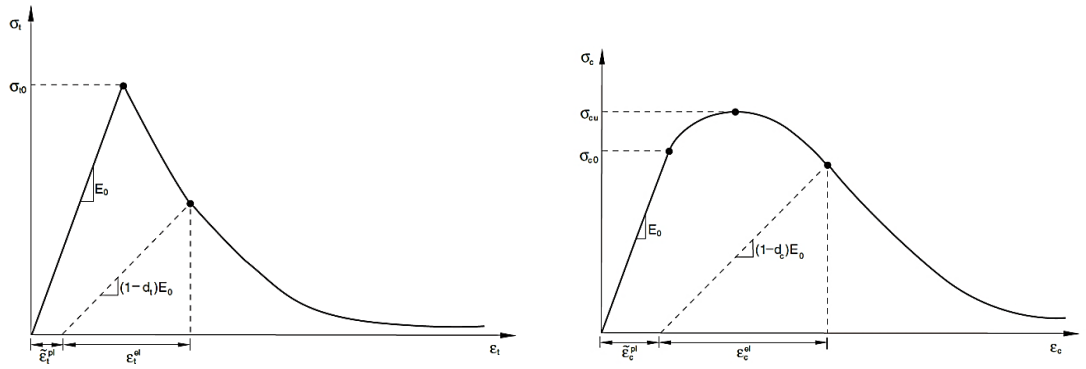

(a) (b)

Figure 2. Response of concrete to (a) uniaxial loading in tension and (b) compression [12]

The main ingredients of the concrete damaged plasticity model are as under:
Strain rate decomposition is assumed for the rate-independent model as given in equation (1).

$$\dot{\varepsilon} = \dot{\varepsilon}^{el} + \dot{\varepsilon}^{pl} \tag{1}$$

where $\dot{\varepsilon}$ is the total strain rate , $\dot{\varepsilon}^{el}$ is the elastic part of the strain rate, and $\dot{\varepsilon}^{pl}$ is the plastic part of the strain rate.
The stress-strain relations are governed by scalar damaged elasticity:

$$\begin{aligned} \sigma &= (1-d)D_0^{el} : \left(\varepsilon - \varepsilon^{pl}\right) \\ &= D^{el} : \left(\varepsilon - \varepsilon^{pl}\right) \end{aligned} \tag{2}$$

where D_0^{el} is the initial (undamaged) elastic stiffness of the material; $D^{el} = (1-d)D_0^{el}$ is the degraded elastic stiffness; and d is the scalar stiffness degradation variable, which can have values in the range from zero to one for undamaged material and fully damaged material. Therefore reduction in the elastic stiffness occurs during the failure of concrete in cracking or crushing. According to the scalar-damage theory, the stiffness degradation is isotropic and characterized by a degradation variable, d. Thus using the concept of continuum damage mechanics, the effective stress can be defined as

$$\overline{\boldsymbol{\sigma}} \overset{\text{def}}{=} \boldsymbol{D}_0^{el} : \left(\boldsymbol{\varepsilon} - \boldsymbol{\varepsilon}^{\boldsymbol{pl}}\right) \tag{3}$$

The Cauchy stress is related to the effective stress through the scalar degradation relation:

$$\boldsymbol{\sigma} = (1-d)\overline{\boldsymbol{\sigma}} \tag{4}$$

The factor $(1-d)$ is the ratio of the effective load-carrying area to the total section area .If the damage is not considered i.e. d = 0, then the stress $\overline{\sigma}$ is equivalent to Cauchy stress σ. On the occurrence of damage, the external loads are being resisted by the effective area hence the effective stress becomes more representative then the Cauchy stress [12]. As explained by in [11] and [13] and stated in the ABAQUS theory manual the degradation variables are governed by a set of hardening variable $\tilde{\varepsilon}^{pl}$, and the effective stress; that is $d = d\left(\sigma, \tilde{\varepsilon}^{pl}\right)$.
The conversion of uniaxial stress-strain curve to stress to plastic strain curve is assumed in the form

$$\sigma_t = \sigma_t\left(\tilde{\varepsilon}_t^{pl}, \dot{\tilde{\varepsilon}}_t^{pl}, \theta, f_i\right) \tag{5a}$$

$$\sigma_c = \sigma_c\left(\tilde{\varepsilon}_c^{pl}, \dot{\tilde{\varepsilon}}_c^{pl}, \theta, f_i\right) \tag{5b}$$

where subscripts t and c refers to tension and compression respectively; $\dot{\tilde{\varepsilon}}_t^{pl}$ and $\dot{\tilde{\varepsilon}}_c^{pl}$ are the equivalent plastic strain rates, $\tilde{\varepsilon}_t^{pl} = \int_0^t \dot{\tilde{\varepsilon}}_t^{pl}\, dt$ and $\tilde{\varepsilon}_c^{pl} = \int_0^t \dot{\tilde{\varepsilon}}_c^{pl}\, dt$ are the equivalent plastic strains, θ is the temperature and $f_i, (i = 1,2,..)$ are other predefined field variables [12].

The unloading response is observed to be weakened, when the concrete specimen is unloaded from any point on the strain softening branch of stress-strain curve as shown in Figure 2. It clearly shows that the elastic stiffness of the material is degraded. The degradation of elastic stiffness under tension and compression is considerably different. In either case the effect is noticeable with the increase in plastic strain. Two damage variables, d_t and d_c are assumed to define this degraded response of concrete, which are, as stated before, assumed to be functions of plastic strains, temperature, and field variables [12].

$$d_t = d_t\left(\tilde{\varepsilon}_t^{pl}, \theta, f_i\right), \ \ (0 \le d_t \le 1) \tag{6a}$$

$$d_c = d_c\left(\tilde{\varepsilon}_c^{pl}, \theta, f_i\right), \ \ (0 \le d_c \le 1) \tag{6b}$$

The values of uniaxial degradation variables increase in accordance with the equivalent plastic strains. If E_0 is the initial undamaged elastic stiffness of concrete, then the values of the damage variables range between zero and one, for undamaged and fully damaged material respectively [12]. From Figure 2,

$$\sigma_t = (1 - d_t)E_0\left(\varepsilon_t - \tilde{\varepsilon}_t^{pl}\right) \tag{7a}$$

$$\sigma_c = (1 - d_c)E_0\left(\varepsilon_c - \tilde{\varepsilon}_c^{pl}\right) \tag{7b}$$

From the above explanation it is clear that to calculate the effective stress, which will be supplied as an input in the form of material property for the analysis, is fully dependent on the degradation parameter 'd'.

2.1.2 Constitutive Relationship:

***(a) Concrete in compression*:**

The stress-strain relation of the concrete is modelled as described by Eq. (8), as in [14].

$$\sigma = \frac{E_c \varepsilon}{1 + \left(\frac{\varepsilon}{\varepsilon_0}\right)^2} \tag{8a}$$

$$\varepsilon_0 = \frac{2f_c'}{E_c} \tag{8b}$$

$$E_c = \frac{\sigma}{\varepsilon} \tag{8c}$$

where:

σ = stress at any strain ε, MPa

ε = strain at stress σ

ε_0 = strain at the ultimate compressive strength σ_c'

The stress-strain curve of concrete in compression is as shown in Figure 3

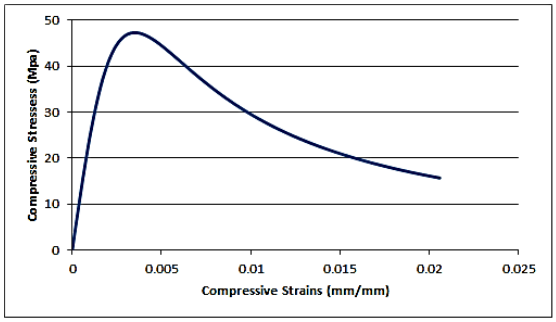

Figure 3. Stress-Strain Curve for Concrete

The damage parameter in compression:

The damage parameter is calculated by using Eq. (9) as described in [15] and [16],

$$d_c = 1 - \frac{\sigma_c E_c^{-1}}{\varepsilon_c^{pl}\left(\frac{1}{b_c} - 1\right) + \sigma_c E_c^{-1}} \tag{9}$$

Where plastic strain ε_c^{pl} is determined proportional to the elastic strain $\varepsilon_c^{in} = \varepsilon_c - \sigma_c E_c^{-1}$ using a constant factor b_c such that $0 < b_c \leq 1$. A value $b_c = 0.7$ is used as suggested in [15].

(b) Concrete in Tension:

The stress-strain curve of concrete in tension is as shown in Figure 4. The ascending and descending parts are obtained by using Eq.(10a) and Eq.(10b) respectively [17].

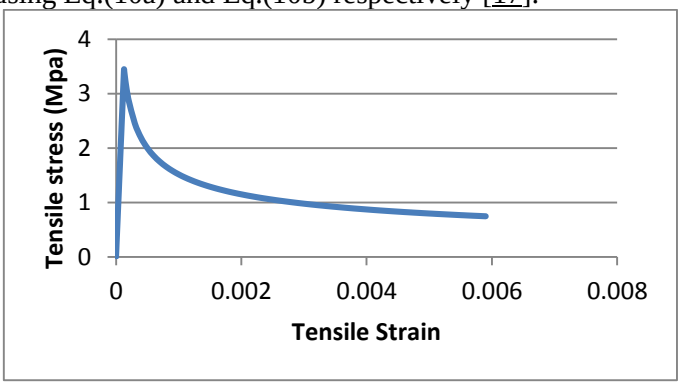

Figure 4. Stress-Strain Curve for concrete in Tension

$$\sigma_t = E_c \varepsilon_t \quad \varepsilon_t \leq \varepsilon_{cr} \tag{10a}$$

$$\sigma_t = \sigma_{cr}\left(\frac{\varepsilon_{cr}}{\varepsilon_t}\right)^{0.4} \quad \varepsilon_t > \varepsilon_{cr} \tag{10b}$$

where E_c is modulus of elasticity of concrete; ε_{cr} is cracking strain of concrete and σ_{cr} is cracking stress of concrete.

The damage parameter in tension: Tension stiffening

The tension stiffening model is assumed as shown in the Figure 5. where ε_0 is estimated using the Eq. (11) given in [18].

$$\varepsilon_0 = \frac{2G_f \cdot ln(3/b)}{\sigma_t \cdot (3 - b)} \tag{11}$$

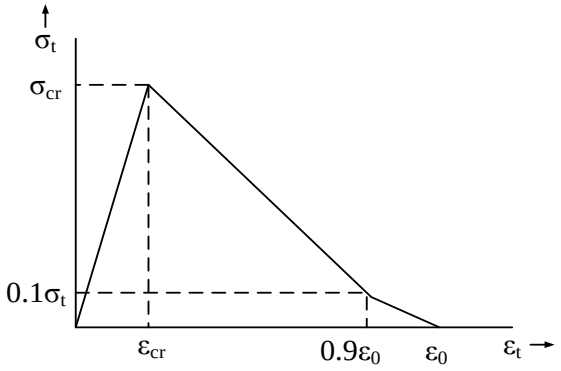

Figure 5. Tension stiffening model

Where G_f is the fracture energy which is dissipated in the formation of a crack of unit length per unit thickness and is considered a material property, and b is element width; all dimensions are in FPS system.

2.2 Reinforcing Steel and Liner plate model:

The reinforcing steel and Liner plate are assumed to behave identical in tension and compression. The stress strain curve for reinforcing steel and liner plate is modelled by using an elasto-plastic material model. The von Mises failure criteria with isotropic hardening are adapted to represent the nonlinear behavior of the material [12].

2.3 Prestressing Steel

The stress–strain curve of prestressing steel strands, Equations (12a) and (12b) are plotted in Figure 6. The Ramberg–Osgood curve is suitable to closely approximate an experimental curve that resembles two straight lines connected by a curved knee. The curvature of the knee is controlled by the shape parameter, a constant m, taken as 4. The first almost straight portion of the Ramberg–Osgood curve is asymptotic to the inclined dotted straight lines with a slope of E'_{ps} at the origin. The modulus E'_{ps}, which is slightly greater than E_{ps}, is determined such that the Ramberg–Osgood curve coincides with the elastic straight line (with slope of E_{ps}) at the point of 0.7 f_{pu} [17].

$$f_p \le 0.7 f_{pu} \qquad f_p = E_{ps}(\varepsilon_{dec} + \varepsilon_s) \tag{12a}$$

$$f_p > 0.7 f_{pu} \qquad f_p = \frac{E'_{ps}(\varepsilon_{dec} + \varepsilon_s)}{\left[1 + \left\{\frac{E'_{ps}(\varepsilon_{dec} + \varepsilon_s)}{f_{pu}}\right\}^m\right]^{\frac{1}{m}}} \tag{12b}$$

Where, f_p = stress in prestressing steel; ε_s = strain in the mild steel; ε_{dec} = strain in prestressing steel at decompression of concrete; E_{ps} = elastic modulus of prestressed steel, E'_{ps} = tangential modulus of Ramberg–Osgood curve at zero load, f_{pu} = ultimate strength of prestressing steel; m = shape parameter.

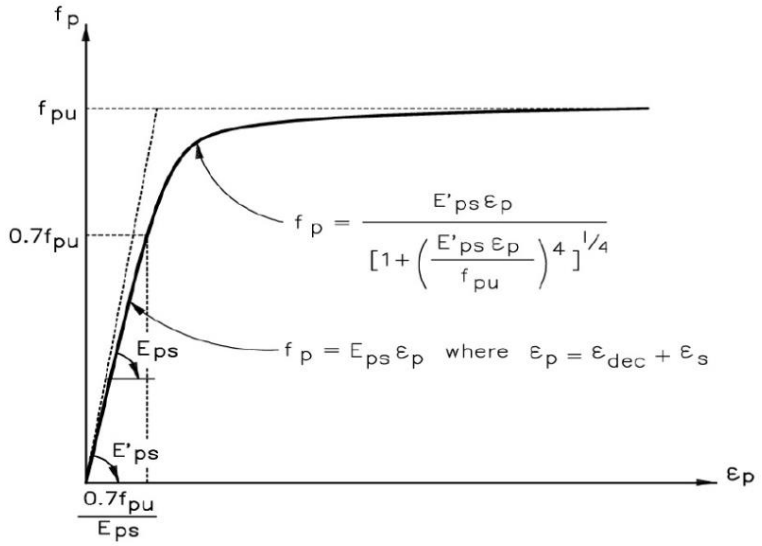

Figure 6. Stress–strain relationship of prestressing strands [17]

2.4 The Material Properties:

In the present finite element analysis the material property data for the concrete is taken for dome and the wall as documented in CSNI report [6]. The material property for reinforcing steel is taken as an average value. The material properties used are as given in Table 1.

Table 1 Material Property

Material	Property	Value
Concrete	Elastic Modulus	26970 MPa
	Uniaxial Compressive Strength	47.30 MPa
	Uniaxial Tensile Strength	3.45 MPa
	Poisson's Ratio	0.18
Reinforcing Steel	Elastic Modulus	1.84E5 MPa
	Yield stress	470 MPa
	Poisson's Ratio	0.3
Liner Plate	Elastic Modulus	218700 MPa
	Yield stress	375.595 MPa
	Poisson's Ratio	0.3
Prestressing Steel	Elastic Modulus	191000 MPa
	Yield stress	1691 MPa
	Elastic Limit Stress	1339 MPa
	Ultimate Strength	1912 MPa
	Poisson's Ratio	0.3

2.5 The Riks Method for Nonlinear Analysis:

The nonlinear solutions are generally been evaluated by Newton-Raphson method and its modifications. But the iteration procedure diverges near limit points as shown in Figure 7, as in the neighborhood of a limit point the tangent matrix $[K_T]$ becomes singular. Riks and Wempner suggested a procedure to predict the nonlinear equilibrium path through limit points. The method provides a technique to control progress along the equilibrium path for the Newton-Raphson method and its modifications. The load increment for each load step is considered to be an unknown and solved as a part of the solution [19].

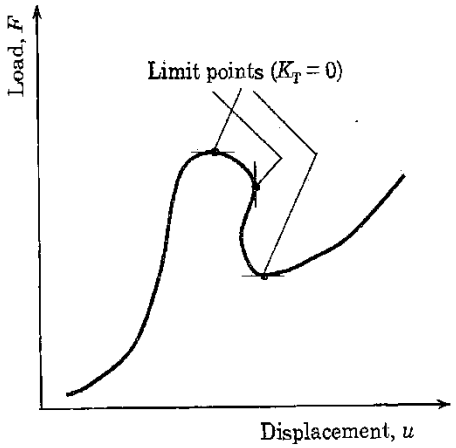

Figure 7. Load-deflection curve with limit points [20]

In [20] the author has explained the basic idea of the Riks technique for a single nonlinear equation. The length Δs of the tangent to the current equilibrium point is prescribed, and the new point is found as the intersection of the normal to the tangent with the equilibrium path as shown in Figure 8a. Then iteration is performed along the normal toward the new equilibrium point. Figure 8b shows the use of a circular arc instead of the normal, as suggested in [19], with Δs as its radius and the current equilibrium point as the center of the circle.

For multidimensional problems the normal and circular arcs become a plane and sphere, respectively, as shown in [19] where the author updated the tangent stiffness matrix only at the beginning of each load increment (i.e. modified Newton-Raphson method).

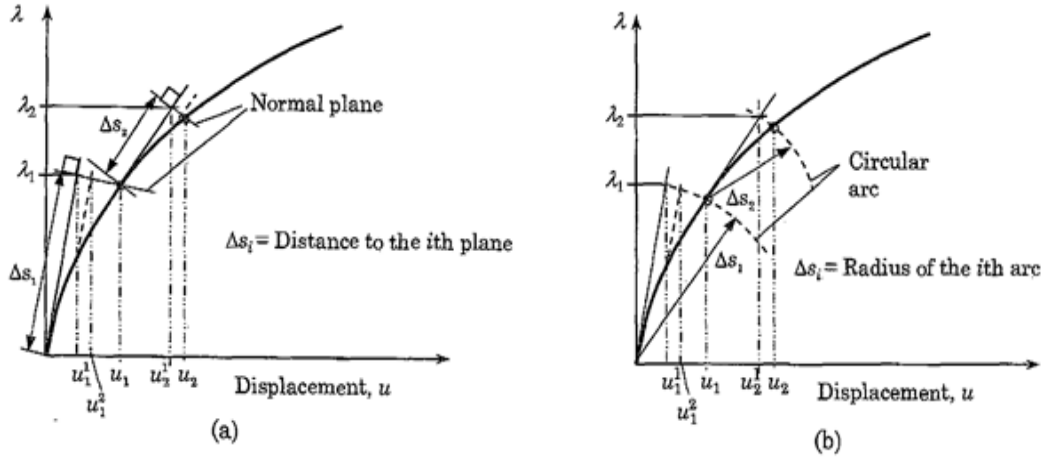

Figure 8 The Riks scheme. (a) Normal plane method. (b) Circular arc method [20]

III. THE FINITE ELEMENT MODEL

The present 1/8th model consists of 1548 C3D8 solid element to model concrete wall, basemat and the dome. It is very cumbersome to model each rebar and tendon and to place at its appropriate location in the model. Hence in this study it is proposed to use the facility provided in ABAQUS to define the rebar as the section property through membrane. The reinforcement and the prestressing tendons are modelled using membrane section facility to define rebar. The inner and outer hoop rebar layers are modelled with 335 and 353 numbers of M3D4 element respectively and the inner and outer meridional rebar layers are modelled with 384 and 353 numbers of M3D4 element respectively. Also the prestressing tendons, hoop and meridional are modelled with 353 and 344 numbers of M3D4 elements respectively. The liner also is modelled as membrane with 337 numbers of M3D4 elements. The rebars and the tendons modelled as membrane then embedded into the main model. The liner is

connected to the concrete wall through tie constraint to ensure the perfect connection between concrete wall and the liner.

Figure 9 shows the finite element meshed 1/8th model of containment structure, also it shows the internal pressure applied to the model. Boundary conditions imposed on the symmetry planes are displacements in the circumferential direction, rotation in radial direction and rotation in the z-direction is considered zero. The bottom of the base slab is assumed as fixed and hence Encastre boundary condition is imposed. Figure 9 also shows the boundary conditions. The prestressing force is applied using *INITIAL CONDITION through predefined fields properties. The analysis is performed using ABAQUS/Standard for internal pressure only. Static RIKS method is employed for the analysis.

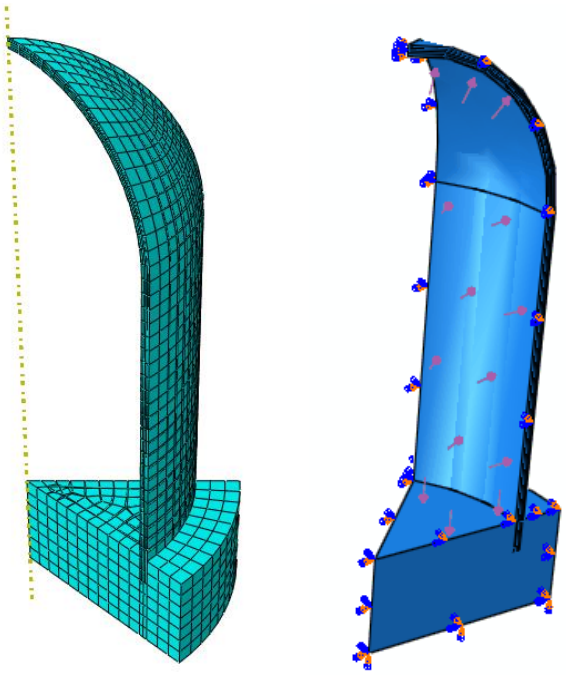

Figure 9. Finite Element Meshed and subjected to internal pressure model

IV. FINITE ELEMENT ANALYSIS RESULTS

The results of Finite element analysis are presented through Figure 10 to 13. The locations chosen for the result are standard locations as described in ISP 48 report [6]. Due to brevity only a few critical locations selected. Figure 10 presents the radial displacement at elevation at 0.0 and at 250 mm above basemat. Figure 11 shows the radial displacement at elevation 6200 mm and at elevation 10750 mm above the basemat, which are well in agreement with the results documented in [21]. It also confirms the nonlinear behaviour. Figure 12 shows the vertical displacement at elevation 0.0 and at elevation 10750 mm above basemat. However Figure 13 shows a good agreement in Rebar Strain in Meridional Direction at EL 250 mm above basemat (Inner Rebar Layer) and Rebar Strain in Meridional Direction at EL 250 mm above basemat (Outer Rebar Layer).

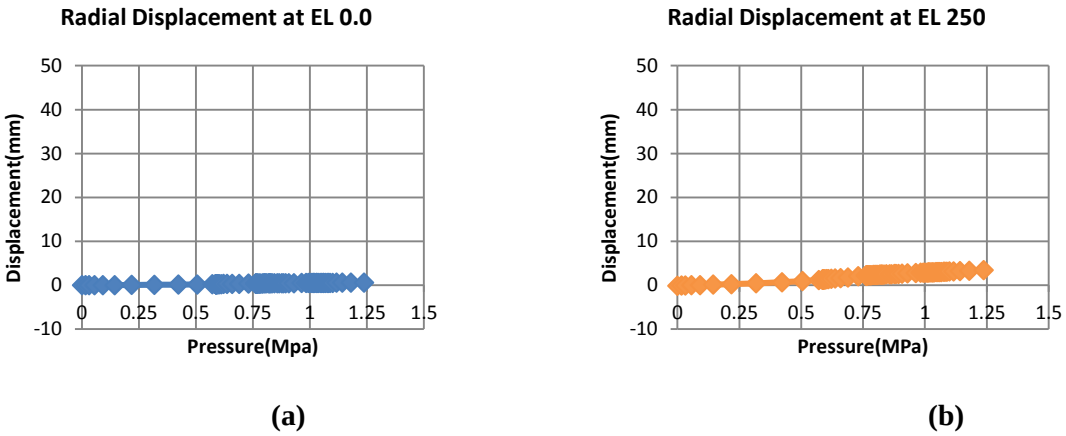

Figure 10. Radial Displacement at EL 0.0 and 250 mm above basemat

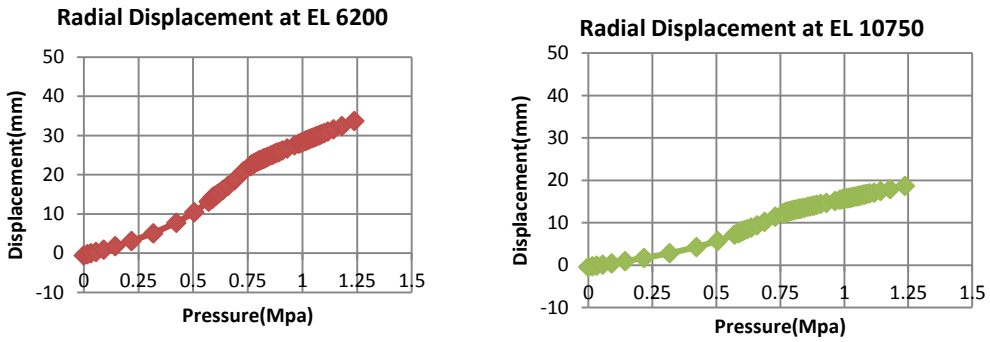

Figure 11. Radial displacement at EL 6200 mm and EL 10750 mm above basemat

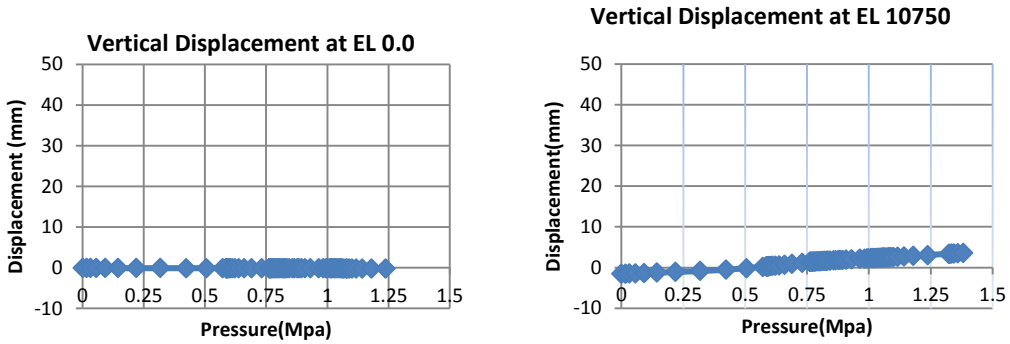

Figure 12. Vertical displacement at EL 0.0 mm and EL 10750 above basemat

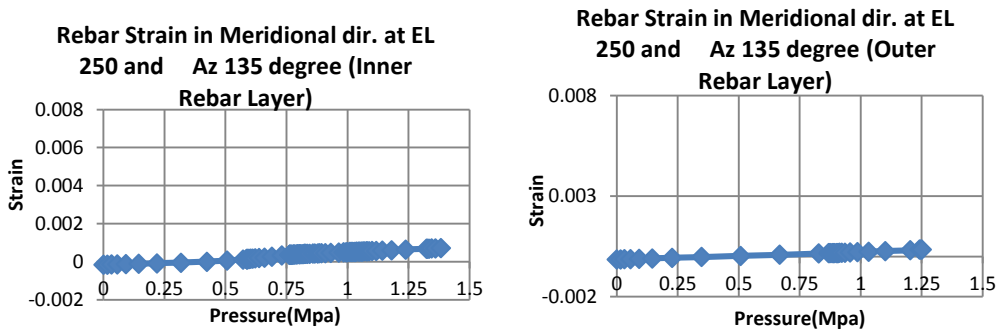

(Inner Reabar Layer) (Outer Reabar Layer)

Figure 13. Rebar Strain in Meridional Direction at EL 250 mm above basemat

V. CONCLUSION

In this study, the results of the nonlinear finite element analysis of a 1/8th model of 1:4 scaled model of prestressed concrete containment vessel, leads to following conclusions:

a) The procedure followed for representing the reinforcing steel and the prestressing tendons through the membrane property have shown similar behavior as that would have shown by modelling them as individual rebar.
b) The constitutive models of the materials introduced are capable of taking care of the instability in solution up to LST pressure capacity.
c) The displacements obtained are at the pressure almost 3 times greater than Pd = 0.39 MPa, where Pd is the design pressure for containment model.
d) The quick and reliable estimation of pressure capacity of the containment structure can be obtained by this procedure.
e) As the temperature effect is not considered for the present study, however it can be incorporated by considering the thermal loading.
f) The analysis can be extended till the structural failure mode test.

ACKNOWLEDGEMENT

This work is supported by Department of Structural Engineering, Veermata Jijabai Technological Institute, Matunga, Mumbai.

REFERENCES

[1] D. W. Halligan, "Structural design criteria for secondary containment structures," *Nuclear erinngineeg and design*, vol. 8, pp. 427-434, June 1968.

[2] D.W. Murray, "Observations on analysis, testing and failure of prestressed concrete containments," *Nuclear Engineering and Design*, pp. 37-46, 1984.

[3] D.S. Horschel, "Construction Of A 1/6-Scale Concrete Containment Model," *Nuclear Engineering And Design*, pp. 341-347, 1987.

[4] P P. Shunmugavel And O. Gurbuz, "An Evaluation Of Structural Failure Modes For Prestressed Concrete Containments," *Nuclear Engineering And Design*, pp. 349-355, 1987.

[5] Y. Bangash, *Containment Vessel Design AND Practice*.: Progress in Nuclear Energy, 1983, vol. II.

[6] NEA/CSNI/R(2005)5/Vol1, "International Standard Problem No. 48 Containment Capacity,".

[7] V. K Luk, "Pretest Round Robin Analyses of a Prestressed Concrete Containment Vessel Model," Albuquerque, NM: Sandia National Laboratories, August, 2000.

[8] Y. R. Rashid , V. K. Luk and M. F. Hessheimer R. A. Dameron, "“Pretest Analysis Of A 1:4-Scale Prestressed Concrete Containment Vessel Model”," Washington DC, August 2001.

[9] E. W. Klamerus, L. D. Lambert, G. S. Rightley, R. A. Dameron M. F. Hessheimer, "Overpressurization Test of a 1:4-Scale Prestressed Concrete Containment Vessel Model," Albuquerque, NM, NUREG/CR-

6810, SAND2003-0840P, March 2003.

[10] Y. R. Rashid, and M. F. Hessheimer R. A. Dameron, "Posttest Analysis of a 1:4-Scale Prestressed Concrete Containment Vessel Model," Prague, Czech Republic, August 17 –22, 2003.

[11] Jeeho Lee and Gregory L. Fenves, "Plastic-Damage Model For Cyclic Loading of Concrete Sructures," *Journal of Engineering Mechanics, ASCE*, vol. Vol. 124, no. No. 8, pp. Vol.124, No. 8, pp. 882-900., August 1998.

[12] *Abaqus Analysis User's Manual 6.12*.: Dassault Systèmes Simulia Corp., Providence, RI, USA, 2012.

[13] S.Oller, E.Onate Lubliner J and J.Oliver, "A plastc-damage model for concrete," *Int. J. Solids Structures*, vol. 25, no. 3, pp. 299-326, 1989.

[14] J.G. MacGregor, *Reinforced concrete mechanics and design*.: Prentice-Hall, Inc, Englewood Cliffs, NJ, 1992.

[15] V., Mark, P. Birtel, "Parameterised Finite Element Modelling of RC Beam Shear Failure," in *ABAQUS Users' Conference*, Cambridge, Massachusetts, USA, 2006, pp. 95-108.

[16] Michel Bender Peter Mark, "Computational modelling of failure mechanisms in reinforced concrete structures," *Scientific Journal Facta Universitatis, Series: Architecture and Civil Engineering*, vol. 8, no. 1, pp. 1-12, March 2010.

[17] Hsu Thomas T.C. and Y.L.Mo, *Unified thery of concrete structures*. United Kingdom: John Wiley & Sons, Ltd, 2010.

[18] Kwak Hyo-Gyoung and Filip C.Filippou, "Finite element analysis of reinforced concrete structures under monotonic loads," Department Of Civil Engineering, University Of California, Berkeley, California, Report No.UCB/SEMM-90/14, November 1990.

[19] M.A. Crisfield, "A fast Incremental/Iterative solution procedure that handles snap through," *Computers and Structures*, vol. Vol 13, pp. 55-62, April 1981.

[20] J.N. Reddy, *An Introduction to Nonlinear Finite Element Analysis*, Reprint ed.: Oxford University Press, 2004.

[21] T. Kawasato, A. Kato, A. Shimizu, T. Ogata, Y. Hino, T. Kitani and Y. Murazumi M. Ohba, "Analysis results of a 1:4-scale prestressed concrete containment vessel subjected to pressure and thermal loading," NEA/CSNI/R(2005)5, 2005.

AUTHORS

S V Chaudhari has completed B. E in Civil Engineering in 1986 from Karnataka University. He completed Masters in Structural Engg in 1991 from Gulbarga. University, Karnataka. He joined RGIT, Mumbai as an assistant professor in 1998. Further he joined Ph. D. program at VJTI, Mumbai. Currently he is working as an Associate Professor in the Rajiv Gandhi Institute of Technology, Mumbai.

M A Chakrabati has completed B.E. in Civil Engineering in 1981 and Masters in Structural Engineering in 1985 from VJTI, Matunga, Mumbai. Then she joined VJTI as teaching faculty in 1986. Further she did Ph.D. from IIT Bombay in 1995. Her areas of specialization are Nonlinear analysis of Structures and Earthquake Engineering. Currently she is working as a Professor in Structural Engineering Department, VJTI, Matunga, Mumbai.